

Electronic Supplementary Information for Penta-Pt₂N₄: an ideal two-dimensional material for nanoelectronics

Zhao Liu,^{‡a} Haidi Wang,^{‡a,b} Jiuyu Sun,^a Rujie Sun,^c Z. F. Wang,^{*a,d} and Jinlong Yang^{*a,e}

^a Hefei National Laboratory for Physical Sciences at the Microscale, University of Science and Technology of China, Hefei, Anhui 230026, China

^b Department of Physics and Astronomy, Iowa State University, Ames, IA50011, USA

^c Wavetronix LLC, Provo, Utah 84606, USA

^d CAS Key Laboratory of Strongly-Coupled Quantum Matter Physics, University of Science and Technology of China, Hefei, Anhui 230026, China

^e Synergetic Innovation Center of Quantum Information and Quantum Physics, University of Science and Technology of China, Hefei, Anhui 230026, China

[‡]These authors contributed equally to this work.

*Email: zfwang15@ustc.edu.cn and jlyang@ustc.edu.cn

1, Properties of N₂, N₂H₂, N₂H₄

For N₂, N₂H₂ and N₂H₄ molecules, DFT calculations are carried out by using the Gaussian 09 package¹ with M062X²/BSI level of theory and basis set of 6-31G(p) for N and H atoms.

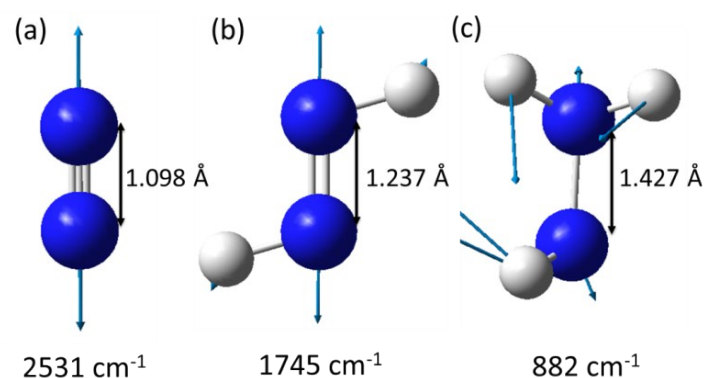


Figure S1. Atomic structure, bond length and characteristic nitrogen dimer vibration frequency of (a) N₂, (b) N₂H₂ and (c) N₂H₄.

The atomic structure, bond length and characteristic nitrogen dimer vibration frequency of these three molecules are shown in Fig. S1. The corresponding electronic configurations of N_2 and N_2H_2 molecules are shown in Fig. S2. One can see the energy of $2s$ electrons are too low to participate in the formation of $3\sigma_g$ and $3\sigma_u$ orbitals. Therefore, the sp^2 hybridization is negligible in both N_2 and N_2H_2 .

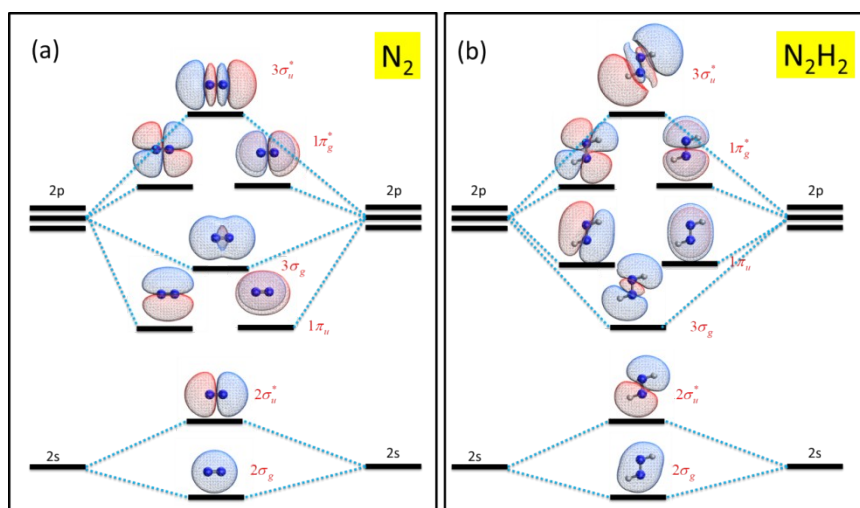


Figure S2. Orbital orders of (a) N_2 and (b) N_2H_4 . The lowest $1\sigma_g$, $1\sigma_u$ orbitals formed by $1s$ electrons are omitted.

2, Effect of hybrid functional on the band structure of Penta-Pt₂N₄

Aligning VBM or CBM together, the PBE and HSE band structures without and with SOC are shown in Fig. S3(a) and (b). Clearly, the band dispersion near VBM and CBM is the same for PBE and HSE band structures. Furthermore, the orbital projected HSE band structures are shown Fig. S3(c). Comparing Fig. S3(c) with Fig.

4(a), one notices that band compositions are also the same for PBE and HSE band structures. Therefore, the effect of hybrid functional on the band structure is rigid, namely, it just corrects the band energy but without changing the band dispersion and band composition near VBM and CBM. Consequently, HSE will not change the carrier mobility results obtained from the PBE+SOC calculations.

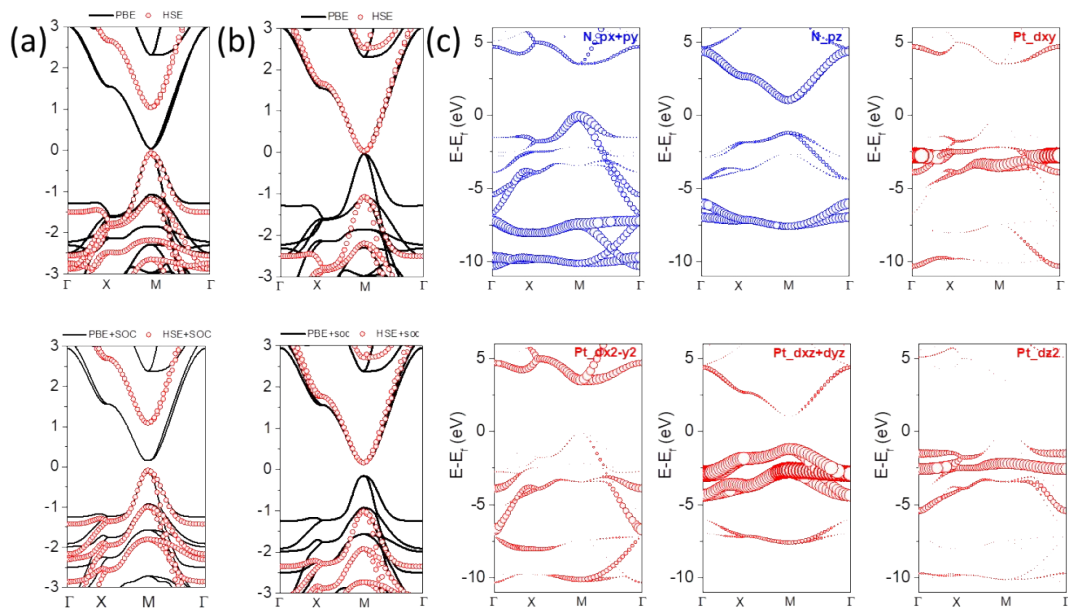


Figure S3. (a) PBE and HSE band structure of Penta-Pt₂N₄ without (top panel) and with (bottom panel) SOC with VBM aligned. (b) PBE and HSE band structure of Penta-Pt₂N₄ without (top panel) and with (bottom panel) SOC with CBM aligned. (c) Orbital projected HSE band structure of Penta-Pt₂N₄.

3, Elastic properties of Penta-Pt₂N₄

The calculated four independent elastic constants of Penta-Pt₂N₄ are listed in Table S1.

These elastic constants satisfy the mechanical stability criteria for tetragonal 2D

materials ($C_{11}C_{22}-C_{12}^2>0$, $C_{66}>0$), indicating Penta-Pt₂N₄ to be mechanically stable.

Table S1. Four independent elastic constants of Penta-Pt₂N₄.

Elastic constant	C ₁₁	C ₂₂	C ₆₆	C ₁₂
GPa	722	722	152	127

4, Molecular adsorption on Penta-Pt₂N₄

Typical adsorption configurations for different molecules on Penta-Pt₂N₄ are shown in Fig. S4-S8. Three different adsorption sites are chosen: top of N, top of Pt and top of hollow site. For linear molecule of CO₂, H₂, N₂ and O₂, the configurations of molecule parallel and perpendicular to the Penta-Pt₂N₄ plane are considered.

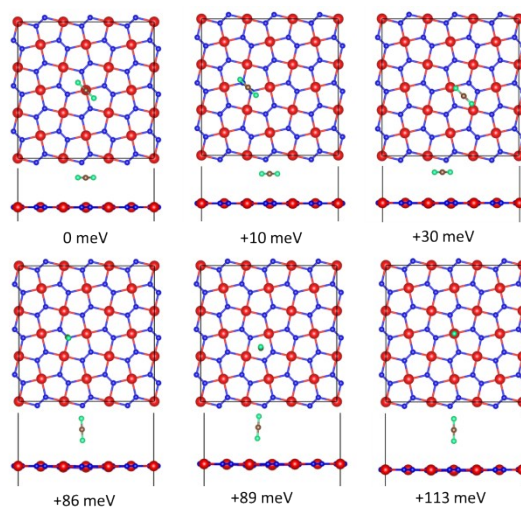


Figure S4. Six typical adsorption configurations of CO₂ on Penta-Pt₂N₄. The energy is relative to the lowest energy configuration.

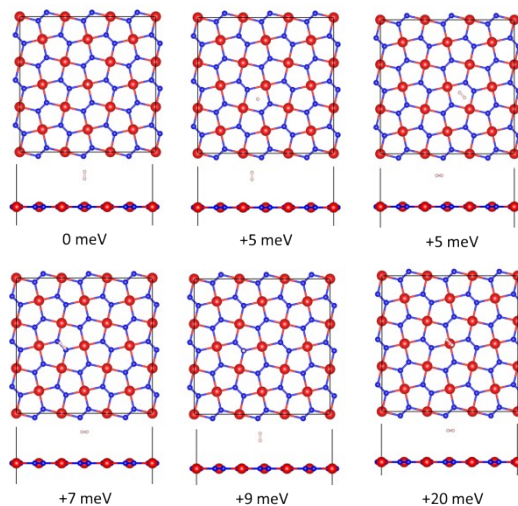


Figure S5. Six typical adsorption configurations of H_2 on Penta- Pt_2N_4 . The energy is relative to the lowest energy configuration.

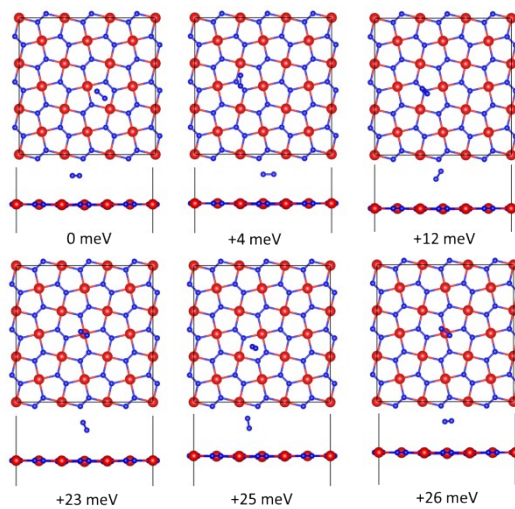


Figure S6. Six typical adsorption configurations of N_2 on Penta- Pt_2N_4 . The energy is relative to the lowest energy configuration.

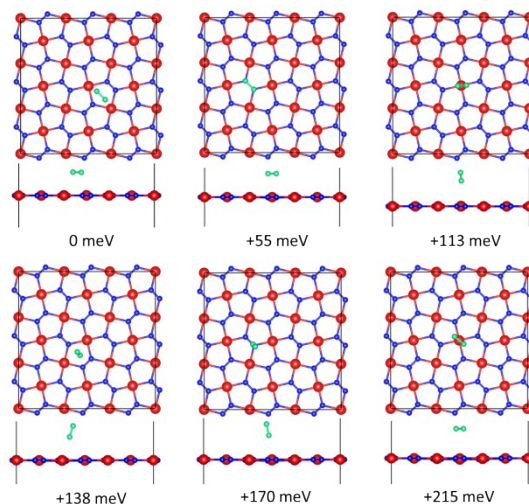


Figure S7. Six typical adsorption configurations of O_2 on Penta- Pt_2N_4 . The energy is relative to the lowest energy configuration.

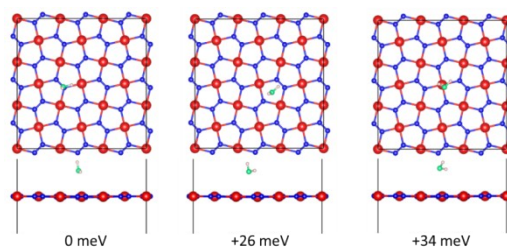


Figure S8. Three typical adsorption configurations of H_2O on Penta- Pt_2N_4 . The energy is relative to the lowest energy configuration.

5, Orbital coupling diagram

At the Γ point, four states of Penta- Pt_2N_4 are plotted to illustrate the orbital coupling between d orbitals of Pt atoms and p orbitals of N atoms, as discussed in the main manuscript.

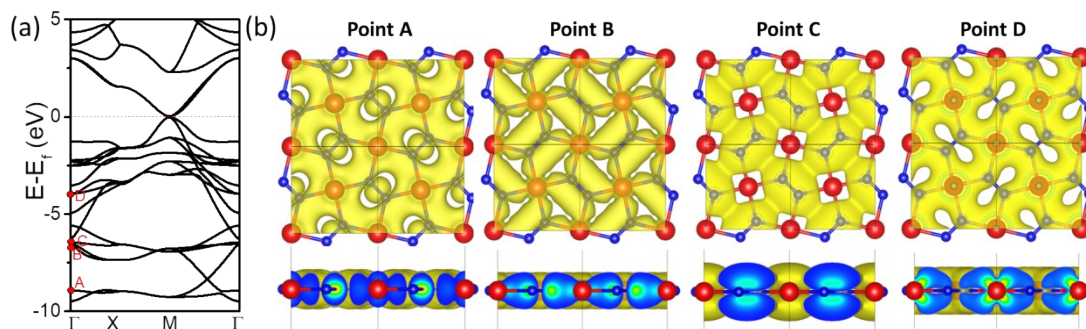


Figure S9. (a) PBE band structure with four states labeled as A, B, C and D at Γ point.

(b) Partial charge density of state A, B, C and D labeled in (a).

6, Properties of Penta-Ni₂N₄ and Penta-Pd₂N₄

All Penta-X₂N₄ have the same space group and their basic structure parameters are listed in Table S2.

Table S2. Lattice constant (a), bond length of nitrogen dimer (N=N) and metal-nitrogen (M-N) for three different Penta-M₂N₄ structures.

Parameter	Penta-Ni ₂ N ₄	Penta-Pd ₂ N ₄	Penta-Pt ₂ N ₄
a (Å)	4.53	4.87	4.80
N=N (Å)	1.24	1.22	1.26
M-N (Å)	1.88	2.05	2.00

The PBE and HSE band structures of Penta-Ni₂N₄ and Penta-Pd₂N₄ are shown in Fig. S10(a) and (e), respectively. The HSE has a rigid effect on the band structure, which corrects the band gap to 0.84 and 1.03 eV for Penta-Ni₂N₄ and Penta-Pd₂N₄,

respectively. The phonon spectrum of Penta-Ni₂N₄ and Penta-Pd₂N₄ are shown in Fig. S10(b) and (f), respectively. The characteristic vibration frequency of N=N is 1470 cm⁻¹ and 1500 cm⁻¹ in Penta-Ni₂N₄ and Penta-Pd₂N₄, respectively. This value is slight larger than that in Penta-Pt₂N₄, indicating a larger modulus. AIMD simulations for Penta-Ni₂N₄ and Penta-Pd₂N₄ are shown in Fig. S10(c) and (g), respectively. The fluctuation of total energy is very small, within 0.1 eV in the time scale of 5 ps. The snapshots taken at 5 ps display a stable structure for both Penta-Ni₂N₄ and Penta-Pd₂N₄, as shown in Fig. 10(d) and (h), respectively. Additionally, the nitrogen dimers are still in the double bond range in our calculations.

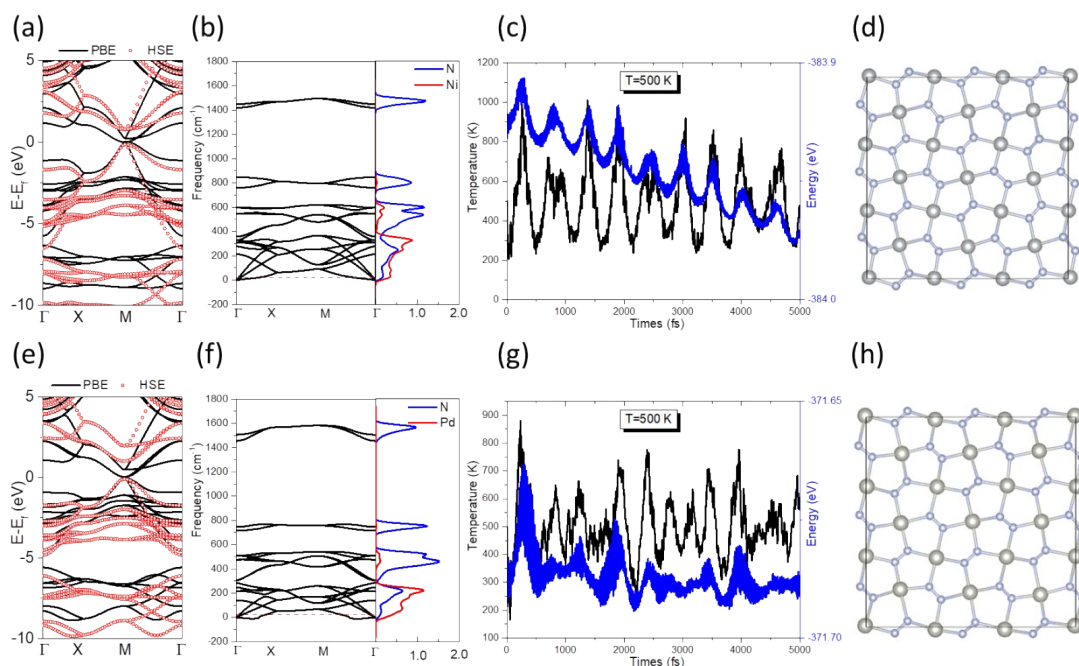


Figure S10. (a) PBE and HSE band structures of Penta-Ni₂N₄. (b) Phonon spectrum and partial density of state of Penta-Ni₂N₄. (c) Fluctuation of temperature and total energy at 500 K in AIMD simulation of Penta-Ni₂N₄. (d) The snapshot taken at the

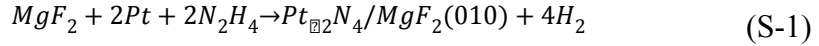
end of AIMD calculation in (c). (e)-(h) are the same to (a)-(d), but for Penta-Pd₂N₄.

7, Details of the proposed CVD/MBE synthesis method

Table S3. DFT lattice constants of Penta-Pt₂N₄, MgF₂(010) substrate and Penta-Pt₂N₄/MgF₂(010), layer distance and adsorption energy between Pt₂N₄ and MgF₂(010).

Functional	Lattice parameters(Å)			Layer distance (Å)	Absorption energy(eV/atom)
	Pt ₂ N ₄	MgF ₂	Pt ₂ N ₄ /MgF ₂		
PBE	4.804	4.646	/	/	/
PBE+D3	4.810	4.619	4.745	2.780	0.011

N₂H₄ as nitrogen resource:



Gibbs free energy of H₂ under any temperature and pressure:

$$G_{H_2}(T,P) = E_{H_2} + \tilde{\mu}_{H_2}(T,p_0) + k_B T \ln \frac{p_{H_2}}{p_0} \quad (S-2)$$

Gibbs free energy of N₂H₄ under any temperature and pressure:

$$G_{N_2H_4}(T,P) = E_{N_2H_4} + \tilde{\mu}_{N_2H_4}(T,p_0) + k_B T \ln \frac{p_{N_2H_4}}{p_0} \quad (S-3)$$

Gibbs free energy change in the above reaction:

$$\Delta G = G(Pt_{\square 2}N_4/MgF_2(010)) + 4G(H_2) - 2G(Pt) - 2G(N_2H_4) - G(MgF_2)$$

$$\begin{aligned}
&= G(\text{Pt}_{\text{Pt}_2\text{N}_4}/\text{MgF}_2(010)) - 2G(\text{Pt}) - G(\text{MgF}_2) + 4\left\{E_{\text{H}_2} + \tilde{\mu}_{\text{H}_2}\right. \\
&\quad \left. - 2\{E_{\text{N}_2\text{H}_4} + \tilde{\mu}_{\text{N}_2\text{H}_4}(T, p_0) + k_B T \ln \frac{p_{\text{N}_2\text{H}_4}}{p_0}\}\right\} \\
&= \left(E_{\text{Pt}_{\text{Pt}_2\text{N}_4}/\text{MgF}_2(010)} - 2E_{\text{Pt}} - E_{\text{MgF}_2} + 4E_{\text{H}_2} - 2E_{\text{N}_2\text{H}_4}\right) + \{4\tilde{\mu}_{\text{H}_2} \\
&\quad + 2k_B T \ln \frac{p_{\text{H}_2}}{p_{\text{N}_2\text{H}_4}} + 2k_B T \ln \frac{p_{\text{H}_2}}{p_0}\} \\
&= \Delta E_{\text{DFT}} + \{4\tilde{\mu}_{\text{H}_2}(T, p_0) - 2\tilde{\mu}_{\text{N}_2\text{H}_4}(T, p_0)\} + 2k_B T \ln \chi + 2k_B T \ln \frac{p_{\text{H}_2}}{p_0} \tag{S-4}
\end{aligned}$$

where

$$\Delta E_{\text{DFT}} = E_{\text{Pt}_{\text{Pt}_2\text{N}_4}/\text{MgF}_2(010)} - 2E_{\text{Pt}} - E_{\text{MgF}_2} + 4E_{\text{H}_2} - 2E_{\text{N}_2\text{H}_4} \tag{S-5}$$

$$\chi = \frac{p_{\text{H}_2}}{p_{\text{N}_2\text{H}_4}} \tag{S-6}$$

8, AIMD simulation of Penta-Pt₂N₄/MgF₂(010)

AIMD is performed at 800 K, which is a possible reaction temperature for synthesizing Penta-Pt₂N₄. The fluctuation of temperature and total energy is very small within 5 ps [Fig. S11(a)], showing a stable structure of Penta-Pt₂N₄ on MgF₂(010) substrate [Fig. S11(b)].

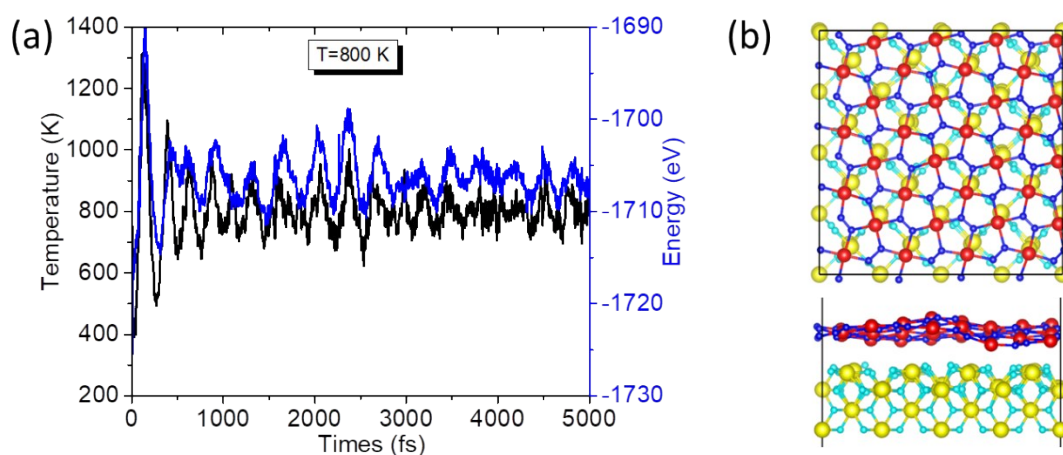


Figure S11. (a) Fluctuation of temperature and total energy at 800 K in AIMD simulation of Penta-Pt₂N₄/MgF₂(010). (b) The snapshot taken at the end of AIMD simulation in (a).

REFERNCES

1. Frisch, M. J. *et al.* Gaussian 09, revision B.01; Gaussian, Inc.: Wallingford, CT, 2009.
2. Zhao, Y. & Truhlar, D. G. The M06 suite of density functional for main group thermochemistry, thermochemical kinetics, noncovalent interactions, excited states, and transition elements: two new functionals and systematic testing of four M06-class functionals and 12 other functionals. *Theor Chem Account* **120**, 215 (2006).